Journal Name

Dynamic Article Links ►

Cite this: DOI: 10.1039/c0xx00000x

www.rsc.org/xxxxxx

ARTICLE TYPE

In-situ observation on the dynamic behaviors of Cu-Al-O_x catalyst for water gas shift reaction during daily start-up and shut-down (DSS)-like operation

Shun Nishimura,[1] Tetsuya Shishido,[2,*] Junya Ohyama,[2] Kentaro Teramura,[2,3] Atsushi Takagaki,[4] Tsunehiro Tanaka,[2] and Kohki Ebitani[1]

Received (in XXX, XXX) Xth XXXXXXXXX 20XX, Accepted Xth XXXXXXXXX 20XX
DOI: 10.1039/b000000x

To compare the catalytic performances against daily start-up and shut-down (DSS) operations between co-precipitated (CP-) and impregnated (IMP-) Cu-Al-O_x catalysts for the water gas shift (WGS) reaction, *in-situ* X-ray adsorption fine structure (XAFS) measurements, temperature-programed reduction (TPR) profiles, X-ray diffraction (XRD) patterns and high resolution transition electron microscope with an energy dispersive X-ray spectroscopy (TEM-EDS) analysis were performed. *In-situ* XAFS studies clearly indicated that the Cu species were frequently oxidized and reduced during DSS operations with steam treatment (DSS-like operation). Based on *in-situ* XAFS and H_2-TPR profiles, the highly active and stable CP-catalyst possessed more susceptible Cu particles to oxidation/reduction (described as redoxable below) than IMP-catalyst even after the DSS-like operations. Interestingly, the XRD and TEM-EDS analysis observed the small Cu particles which were covered with a card-house structure of the *in-situ* formed boehmite in the case of CP-catalyst after the DSS-like operations. According to these results, we concluded that the superior durability of CP-catalyst against frequent redox changes was attributed to the nanoscale coordination with the *in-situ* formed boehmite structure which preserves the small-redoxable Cu particles.

Introduction

In the past decade, the water gas shift (WGS; $CO + H_2O \rightarrow CO_2 + H_2$) reaction has been paid great attention for the removal of toxic CO from reformed hydrogen gas for residential proton-exchange membrane fuel cell (PEMFC) applications, which is one of the most important clean-alternative energy sources for the future. The CO level, which is increased during the steam reforming (SRM), partial oxidation (POX) or autothermal reforming (ATR) reactions, must be reduced to 20 ppm before feeding to the PEMFC due to poisoning of electrocatalytic activity of the Pt catalyst in the anode. In general, a combination of the WGS reaction ($CO + H_2O \rightarrow CO_2 + H_2$) followed by successive selective oxidation ($2CO + O_2 \rightarrow 2CO_2$) has been considered for effective CO reduction, but the later reaction consumes H_2 through the side reaction ($4H_2 + O_2 \rightarrow 2H_2O$). Therefore, many researchers have pursued a highly active catalyst for WGS reaction towards a beneficial PEMFC energy system.[1]

The daily start-up and shut-down (DSS) operation is essential for the application of the PEMFC energy system to small facilities such as homes, buildings and vehicles. Since frequent DSS operation causes the catalyst to be exposed to many different environments (*ex.* temperature movement, exposure to air and/or condensing steam), deactivation of the catalyst can occur quickly. Therefore, it is necessary to consider different strategies from the traditionally highly-functionalized catalysts under steady-state conditions. To this end, investigation of dynamic behavior of the structure in developing catalysts under the DSS operations will give useful information for considering the new demands against DSS operations.

Many researchers have investigated the deactivation mechanism of ceria-supported noble metal catalysts for WGS reaction such as Pt/CeO_2, Au/CeO_2 and Pd/CeO_2. The formation of carbonates and formates on the surface of not only CeO_2 but also noble metal were observed after deactivation by DSS operation in these cases.[2,3] Some researchers proposed the irreversible over-reduction of CeO_2 was also related to the deactivation mechanism in the presence of excess H_2.[4,5] According to these reports, it was considered that reoxidation treatment with air or oxygen is necessary for regeneration in the case of ceria-supported noble metal catalysts under the DSS operations. In this aspect, addition of O_2 to reaction gas[6] or alkaline metal to catalyst[7] were proposed for improving durability of precious metal catalyst.

In general, Cu-based catalysts have higher activity than noble metal-based catalysts, however, the formers have much lower durability than the latters against DSS operations.[8] Cu-based catalysts are known as very sensitive catalysts against frequent atmosphere changes, therefore they are easily deactivated under DSS operation. The Cu/ZnO type catalysts are the most popular

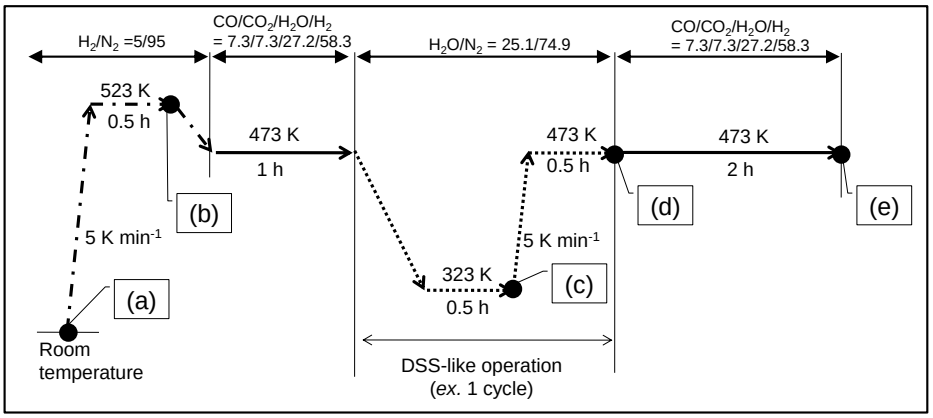

Fig. 1 Diagram of DSS-like operation in the WGS reaction. The (a)-(e) indicate the sampling points for the structural change experiment in Fig. 9.

Cu-based catalysts for WGS reaction, and addition of Al_2O_3, SiO_2 and various alkaline metals,[9-12] investigation for effective supports[13] or optimization of preparation conditions[14,15] has been attempted for improvement of their catalytic performance. Formation of spinel phase was also reported as an effective methodology for high catalytic activity with the Cu-Al, Cu-Fe and Cu-Mn types.[16-19] However, further investigation of competitive Cu-based catalysts is still necessary for mid-and-long term usage. The formation of carbonates,[20,21] passivation by a dense shell of hydroxide[22] and sintering of Cu[23,24] were proposed as the reasons of deactivation in the Cu-based catalyst under DSS operation. Nevertheless, an effective strategy towards a highly durable Cu-based catalyst has not been proposed.

Recently, the formation of the highly active and durable Cu-Al-O_x catalyst prepared by the simple co-precipitation method has been studied under both laboratory and pilot scale DSS conditions over 500 cycles.[24,25] In general, the Cu/Al_2O_3 including ZnO ($Cu/ZnO/Al_2O_3$) catalysts were considered as a standard for Cu-based catalyst for not only the WGS reaction but also the methanol synthesis and SRM reactions because the additive ZnO had a great effects to the activity and durability owing to its spacer and promoter actions, and so on.[26-28] Therefore, the catalytic feature of Cu-Al-O_x catalyst system is an attractive finding. Further elucidation of the novel Cu-Al-O_x catalyst during DSS operations gives valuable information for progressively robust Cu-based catalysts. Herein, we investigated the catalytic dynamic behavior of Cu-Al-O_x catalyst during DSS-like operations using *in-situ* X-ray adsorption fine structure (XAFS) method with combination of other analytical techniques, and revealed the novel roles of the stable Cu-Al-O_x catalyst and deactivation mechanism under the DSS operation.

Experimental

The Cu-Al-O_x catalysts with different durability were prepared by co-precipitation (CP-) and impregnation (IMP-) methods. CP-catalyst was prepared with titration of an aqueous solution of $Cu(NO_3)_2$•$3H_2O$ (8.3 mmol) and $Al(NO_3)_3$•$9H_2O$ (16.6 mmol) to an aqueous solution of Na_2CO_3•$10H_2O$. During titration, pH was adjusted to 9 with an aqueous solution of NaOH. The obtained sky-blue precipitates were aged at 333 K for 24 h, then filtered, washed and dried in oven at 373 K overnight. IMP-catalyst was synthesized from $Cu(NO_3)_2$•$3H_2O$ (4.8 mmol) and 0.5 g of γ-Al_2O_3 (JRC-ALO-8, 164 m^2 g^{-1}) as precursors for metal sources and support, respectively. After drying of water solvent, the residues were dried at 373 K overnight. Each catalyst was calcined at 823 K for 3 h, pressed, crushed and screened to the size between 26 and 42 mesh. The Cu loading in these Cu-Al-O_x catalysts was 5.5 mmol g^{-1} (35 wt%). As the reference catalyst, a commercial $Cu/ZnO/Al_2O_3$ (MDC-7 pellet, Süd-Chemie Co., Ltd., Cu 5.4 mmol g^{-1}) was also screened and applied to the WGS reaction.

These catalysts were tested for WGS reaction in a fixed bed reactor in order to determine their activity and durability under the DSS operations with steam treatment (Figure 1). The as-prepared catalyst (200 mg) was placed between glass-wool. Prior to WGS reaction, catalyst was reduced with a H_2/N_2 (5/95) gas at 523 K for 0.5 h. As the steam treatments, repetitions of temperature between 473 and 323 K under steam flow at the predetermined number of times were performed (denoted as DSS-like operations below). The gas composition (after moving through an ice trap to remove water) was analyzed with an on-line gas chromatograph equipped with a TCD (Molecular Sives-5A column) and a methanizer FID (Porapak-Q column) detectors. Durability of the catalyst was determined to compare their activities before and after DSS-like operations. The gas space velocity per gram catalyst (SV) for WGS reaction was 12.4 L h^{-1} g^{-1}-STP.

X-ray diffraction (XRD) measurement was carried out with a Rigaku RINT 1000 instrument with CuK_α radiation (1.54059 Å) in the range of 2θ = 5-80° with 0.60° min^{-1} scanning rate. The diffraction patterns were analyzed with the database in the JCPDS (Joint Committee of Powder Diffraction Standards). The surface area of prepared catalyst was estimated by the N_2 adsorption method at 77 K using a Brunauer-Emmett-Teller (BET) model in Coulter SA3100. The morphology and elemental distribution were observed by a high resolution transmission electron microscope (HR-TEM, JEOL JEM-2100F) and a scanning TEM with an energy dispersive X-ray spectroscopy (STEM-EDS) attachment. The samples for the TEM measurements were dispersed in water, then the supernatant liquid was dropped onto a carbon coated molybdenum grid and

dried *in vacuo* overnight.

The Cu surface area of the catalyst was determined by N_2O decomposition method at 363 K as described in the previous reports.[29,30] Prior to the measurement, all samples were screened to 26-42 mesh and reduced with a H_2/N_2 (5/95) gas at 523 K for 0.5 h. Temperature-programed reduction (TPR) was performed with an Ohkura BP-2 instrument interfaced with a TCD. The TCD results were normalized to the mass of the used samples, and the rate of H_2 consumption was estimated based on the standard curve of pure CuO (99.999 %, Koujundo Chem. Labo. Co., Ltd.) reduction. Each sample was pre-oxidized under O_2 gas flow at 573 K for 1 h. Then the catalyst was purged with He and cooled to ambient temperature. The TPR profile was recorded under a H_2/Ar (5/95) flow at a ramp rate of 10 K min^{-1}.

In-situ time-resolved Cu K-edge XAFS measurements were carried out at the BL01B1 of SPring-8 with the approval of the Japan Synchrotron Radiation Research Institute (JASRI) (Proposal No. 2008A1170, 2009A1662 and 2009B1690). Double Si(111) single crystals were used for division of energy. In a typical sample preparation, 15 mg of sample was diluted with 16 mg of boron nitride (Wako Pure Chem. Ind. Co., Ltd.), grained and pressed to a pellet. Thereafter, the pellet was placed in the *in-situ* flow cell (ASPF-20-03, Kyowashinku Co., Ltd.) designed by Suzuki and Nomura.[31] The Cu K-edge XAFS spectra were measured for each 60 sec in the range of 8733-10362 eV at intervals of 33 sec for each measurement. The obtained spectra were analyzed with Rigaku REX2000 ver. 2.5.7. software. For deconvolution analysis of the spectra,[32-35] Cu metal, Cu_2O and CuO were used as references for Cu^0, Cu^+ and Cu^{2+}, respectively. The k^3-weighted EXAFS spectra ($k^3\chi(k)$) were obtained from normalized EXAFS spectra, and Fourier-transforms (FTs) of which were performed in the range of k = 3-13 $Å^{-1}$. The coordination numbers (CN) were estimated by curve-fitting analysis with the empirical parameters extracted from Cu foil for the first Cu-Cu shells (2.55 Å); the inverse FTs were performed in the range of k = 4-12 $Å^{-1}$ and R = 1.78-2.61 Å.

Results and Discussion

Figure 2 shows effect of DSS-like operations on CO conversion over WGS reaction for Cu-based catalysts. Commercial MDC-7 ($Cu/ZnO/Al_2O_3$) catalyst showed gradual deactivation by repeated DSS-like operations. The CO conversion of MDC-7 was changed from 59% to 39% before and after 50 cycles of DSS-like operations. Therefore, the scheme of DSS-like operations described in Figure 1 is suitable to evaluate the durability of catalysts. The IMP-catalyst indicated a significant deactivation by DSS-like operations, an alteration from 25% to approximately 2% of CO conversion was observed before and after 10 cycles of DSS-like operations. In contrast, CP-catalyst showed stable catalytic activity even after the DSS-like operations as follows: fresh CP-catalyst possessed 30% conversion, and gradually increased in activity with increasing the cycles of DSS-like operations up to 10 cycles. The structural change, *in-situ* AlOOH

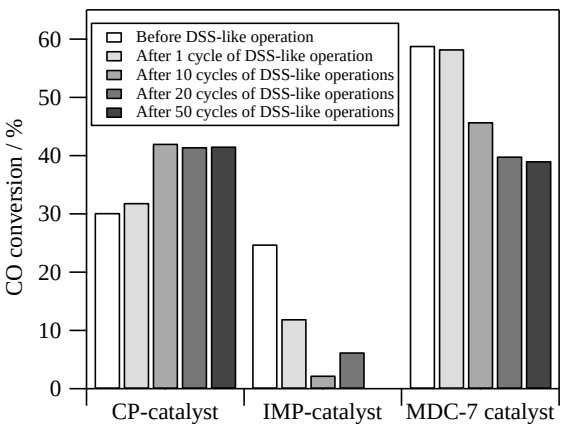

Fig. 2 Effect of DSS-like operations on CO conversion over CP-Cu-Al-O_x, IMP-Cu-Al-O_x and $Cu/ZnO/Al_2O_3$ (MDC-7) catalysts. Reaction temperature 473 K, $CO/CO_2/H_2O/H_2$ = 7.3/7.3/27.2/58.3, SV = 12.4 $Lh^{-1}g^{-1}$.

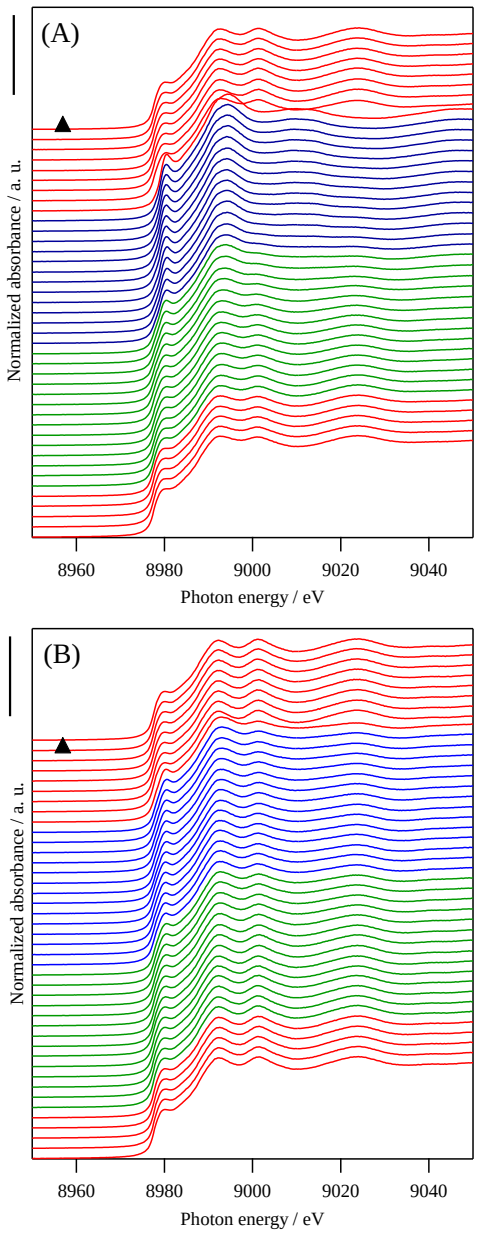

Fig. 3 Changes in XANES spectra over (A) CP-Cu-Al-O_x and (B) IMP-Cu-Al-O_x during 2 cycles of DSS-like operations under the WGS reaction (red lines), 1st and 2nd DSS-like operation (green lines and blue lines).

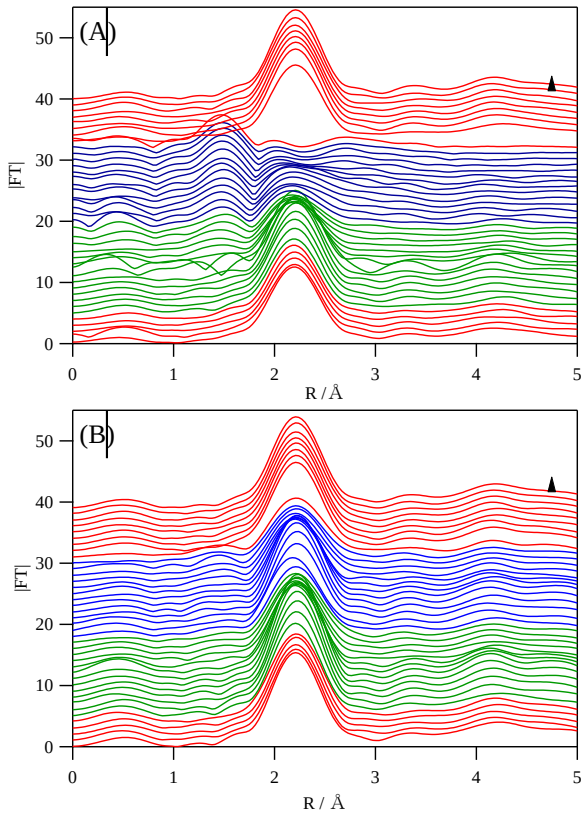

Fig. 4 Changes of |FT| of EXAFS spectra (|FT| of $k^3\chi(k)$) over (A) CP-Cu-Al-O_x and (B) IMP-Cu-Al-O_x during 2 cycles of DSS-like operations under the WGS reaction (red lines), 1st and 2nd DSS-like operation (green lines and blue lines).

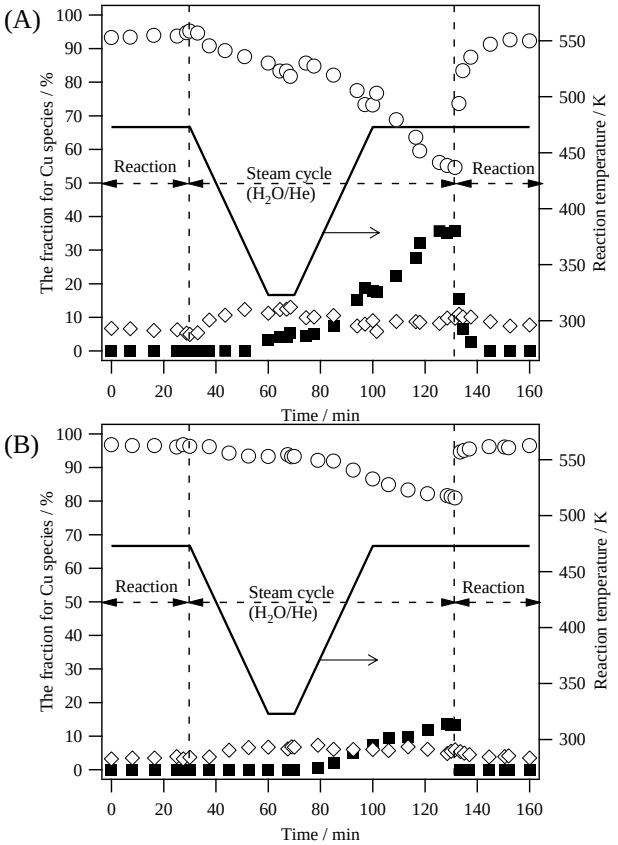

Fig. 5 Fraction of Cu species over (A) CP-Cu-Al-O_x and (B) IMP-Cu-Al-O_x during 1 cycle of DSS-like operation, (open circle) Cu^0, (close square) Cu^+ and (open diamond) Cu^{2+}.

(boehmite) formation during 10 cycles of DSS-like operations resulted in increases in the Cu surface area, BET surface area and the amount of easily reducible Cu species (*vide infra*). As a result, the activity for the CP-catalyst improved gradually from 30 % to 42 %. Above 10 cycles, 42% conversion was maintained over 50 cycles of DSS-like operations. In a comparison of the Cu surface area before and after 10 cycles of DSS-like operations, MDC-7 and IMP- catalysts showed decreases from 18.5 to 10.7 $m^2\ g^{-1}$ and 3.1 to 1.2 $m^2\ g^{-1}$, respectively, whereas the CP-catalyst showed an increase from 9.4 to 11.1 $m^2\ g^{-1}$ (Summarized information was shown in Table S1). It seems that the growth and/or aggregation of Cu particles are attributed to deactivation in the case of MDC-7 and IMP-catalyst, which agrees with the previous reports.[9,11,36,37] However, it is difficult to explain the activity for WGS reaction in terms of only the Cu metal surface area; *ex.* the activities between CP- and IMP- catalysts were 1.2 times differences before DSS-like operations, but the Cu surface area of CP-catalyst was 3 times higher than that of IMP-catalyst at the time. In addition, it is strongly implied that the CP-catalyst has a specific mechanism for inhibition against the aggregation of Cu particles.

To compare the differences between CP- and IMP- catalysts, direct monitoring of Cu species during DSS-like operations was conducted by *in-situ* XAFS measurements. The changes of Cu K-edge (8.98 keV) XANES spectra in each 5 times during 2 cycles of DSS-like operations are described in Figure 3. Both CP- and IMP-catalysts indicated the same tendencies as follows: The two-humped XANES spectra corresponding to Cu metal (Figure S1(A)) were observed during the first reaction (red lines). When steam was introduced during DSS-like operations, the peak intensity around 9000 eV decreased with increasing of the peak intensity around 8990 eV (green and blue lines). These changes were related to the oxidation of Cu^0 to Cu^+ and/or Cu^{2+} species (Figure S1(A)) during the DSS-like operations. Thereafter, the XANES spectra drastically turned to the two-humped spectrum by switching from the steam atmosphere to the reaction. It suggested the immediate reduction from Cu^+ and/or Cu^{2+} species to Cu^0 occurred in the initial stage of the second reaction. For further investigation, |FT| of EXAFS spectra ($k^3\chi(k)$) during 2 cycles of DSS-like operations are shown in Figure 4. The peak at 1.47 Å and 2.24 Å in a normal |FT| correspond to Cu-O (1.86 Å) and Cu-Cu (2.54 Å) after curve fitting, respectively. The positions of these peaks were very close to the first Cu-O shell (1.85 Å) in Cu_2O and the first Cu-Cu shell (2.55 Å) in Cu metal (Figure S1(B)). From the results of |FT| changes, it is clearly indicated that the changes of XANES spectra during DSS-like operations (Figures 3) are associated with the oxidation from Cu metal to Cu_2O, and the remarkable reduction from Cu_2O to Cu metal at the beginning of the second reaction. It is also supposed that the change in XANES spectra of CP-catalyst was much larger than those of IMP-catalyst, indicating that the large part of Cu metal on CP-catalyst was oxidized to copper oxides. These structural alterations during DSS-like operations were also inferable from changes of the k^3-weighted EXAFS spectra

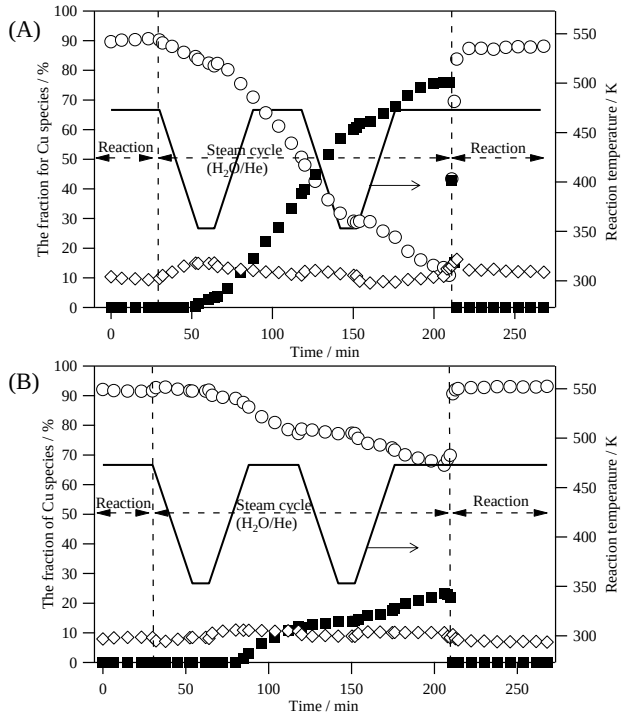

Fig. 6 Fraction of Cu species over (A) CP-Cu-Al-O_x and (B) IMP-Cu-Al-O_x during 2 cycles of DSS-like operations, (open circle) Cu^0, (close square) Cu^+ and (open diamond) Cu^{2+}.

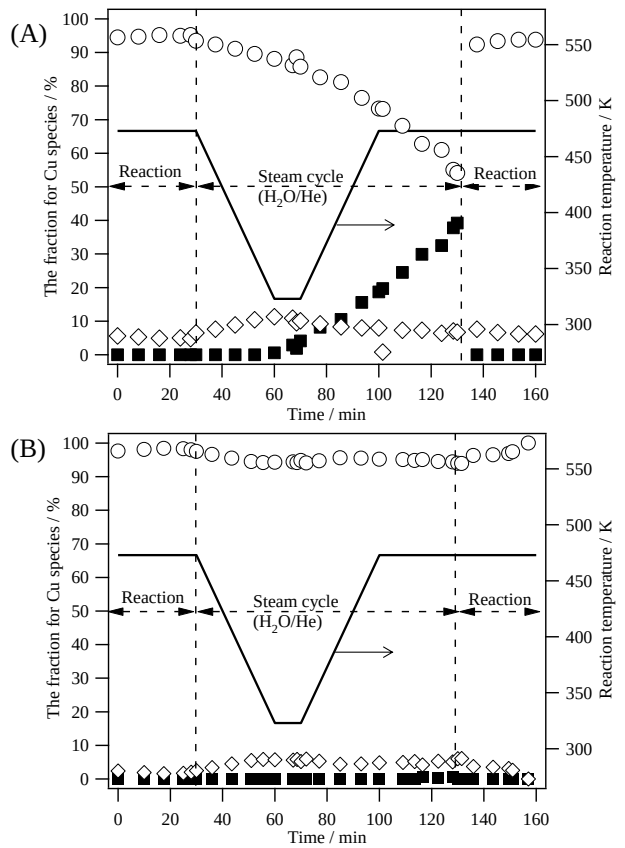

Fig. 7 Fraction of Cu species over (A) prereacted CP-Cu-Al-O_x and (B) prereacted IMP-Cu-Al-O_x during 1 cycle of DSS-like operation, (open circle) Cu^0, (close square) Cu^+ and (open diamond) Cu^{2+}.

(Figure S2 comparing with S1(B)).

To elucidate the changes in Cu species during DSS-like operations, the deconvolution of the obtained XANES spectra were performed using reference XANES spectra (Figure S1(A)) and the estimated fraction for each Cu species was plotted as a function of time. Figures 5 and 6 show the evaluation of the fraction of Cu species during 1 and 2 cycles of DSS-like operations, respectively. Over 90% of Cu species exist as Cu^0 during the first reaction in all cases, then partial oxidation to Cu^+ occurred under DSS-like operations. The oxidation process of Cu^0 to Cu^+ was accelerated by the ramping temperature followed by the drastic reduction of Cu^+ to Cu^0 at the beginning of the second reaction. The partial oxidation of Cu to Cu_2O by water was also proposed by some research groups.[38,39] Although both CP- and IMP- catalysts showed the same redox behavior of Cu species in Figures 5 and 6, the amount of oxidized Cu species in DSS-like operations was much different. The CP-catalyst showed 36% and 76% of Cu^+ species formed in 1 and 2 cycles of DSS-like operations, but the IMP-catalyst possessed 13% and 23% for each. While the temperature of the DSS-like operation is different in Figures 6 and 7, the changes scarcely affected on the evaluations of the amount and the fraction of Cu species during a cycle of DSS-like operation.[40] Changes of the coordination number (CN) of Cu-Cu of 2.54 Å (2.24 Å in a normal |FT|) (Cu metal) indicated that the CP-catalyst has smaller Cu species than the IMP-catalyst during the first reaction before DSS-like operation, but increasing of the coordination number of Cu-Cu estimated by |FT|s, approximately from 10.5 to 12, was observed after repeating 2 cycles of the DSS-like operations in the case of CP-catalyst (Figure S3). The gradual growths of the crystalline of Cu metal in the CP-catalyst after the DSS-like operations were also observed in the XRD patterns (*ex.* the approximate crystalline sizes of Cu(111) were 13 nm (before), 14 nm (after 10 cycles), 16 nm (after 20 cycles), and 23 nm (after 50 cycles)) (Fig. S5(A)) although it exhibited high durability.

We wondered why the CP-catalyst showed good durability even through the growth of Cu metal was suggested by the |FT| and XRD patterns after DSS-like operation. In order to clarify the novel factor of the CP-catalyst, the results of evaluation of the fractions for Cu species using CP- and IMP- catalysts prereacted over 20 cycles of DSS-like operations in the laboratory before XAFS measurement were also investigated (Figure 7). The CP-catalyst prereacted with 20 cycles of DSS-like operations possessing a high activity (42% conv.) shows a similar behavior to the fresh CP-catalyst (Figure 5(A)), and the amount of Cu^+ species (39%) during 1 cycle of DSS-like operation also had a similar value between Figures 5(A) and 7(A). Contrastively, the IMP-catalyst after 20 cycles of DSS-like operations possessing a low activity (6% conv.) drastically decreased the amount of Cu^+ species compared to fresh IMP-catalyst (from 13% to <1%) (Figures 5(B) and 7(B)). These results show that the Cu species in the CP-catalyst kept their original properties in terms of the oxidation after DSS-like operations, however, the IMP-catalyst experienced a big change toward tolerant to oxidation. Comparisons of correlations between CO conversion and the easily-oxidized Cu concentration (Cu^+/Cu^0_{total}) estimated from the XAFS spectra in a cycle of DSS-like operation (described in Figures 5 and 7) were examined. The fresh CP-catalyst indicated

Cu^+/Cu^0_{total} = 3.76×10^{-1} with 30% CO conv. and the prereacted CP-catalyst indicated 4.19×10^{-1} with 42% conv. On the other hand, in the case of IMP-catalyst, the fresh and the prereacted ones showed 1.38×10^{-1} with 25% conv. and 5.13 ×10^{-3} with 6% conv., respectively. These results clearly indicate that the concentration of easily-oxidized Cu species is related to a high catalytic activity of WGS reaction.

Moreover, the fraction of Cu^{2+} (CuO) was flat during DSS-like operations in all cases (Figures 5-7). Thus, the overoxidation of Cu species scarcely occurred in the DSS-like operations. It is known that water could act as an oxidant for Cu metal to Cu_2O ($E^{\circ}(Cu^+/Cu^0)$ = +0.52 V) but could not for Cu_2O to CuO ($E^{\circ}(Cu^{2+}/Cu^+)$ = +0.16 V) because the latter is in range of the stability field of water.[41] Furthermore, Cu^+ has a possibility of transmutation to Cu^{2+} and Cu^0 by disproportionation, however, it seemed to be rare during DSS-like operations. The stable Cu^{2+} species were presumably the hardly accessed CuOs surrounded by Al_xO_y and/or Cu-Al-O_x composite precursors.

In the XAFS results, the DSS operations caused the redox changes of Cu species, gradual oxidation and drastic reduction between Cu metal and Cu_2O, and causing Cu species to grow.

The CP-catalyst suppressed the affects by the redox changes even when it had Cu species susceptible to oxidation. Considering with the results in Figure 2, few changes were observed over 10 cycles of DSS-like operations in cases for both CP- and IMP- catalysts, implied that the oxidation of Cu^0 to Cu_2O was saturated over 10 cycles in the Cu-Al-O_x catalysts in the laboratory reactor. Briefly, the DSS-like operation described in Figure 1 seemed to change the degree for oxidation of Cu metal to Cu_2O in the catalysts, and which was related to the degree for successive reduction from Cu_2O to Cu metal.

To further investigate the redox behavior of CP- and IMP-catalysts, H_2-TPR profiles are measured as shown in Figure 8. All samples were pretreated in O_2 flow at 573 K for 1 h, and then each profile was recorded from 323 K with 10 K min^{-1} under H_2/Ar flow. The H_2-TPR profiles supported the observation of Cu oxides on the sample after each treatment. Calcined CP-catalyst exhibited two peaks around 550 K and 620 K (Figure 8A(a)). After reduction treatment, a single peak around 530 K was observed (Figure 8A(b)). After that, the peak gradually shifted to the lower temperature side with increasing the amount of easily reducible CuO by repeating the DSS-like operations (Figure

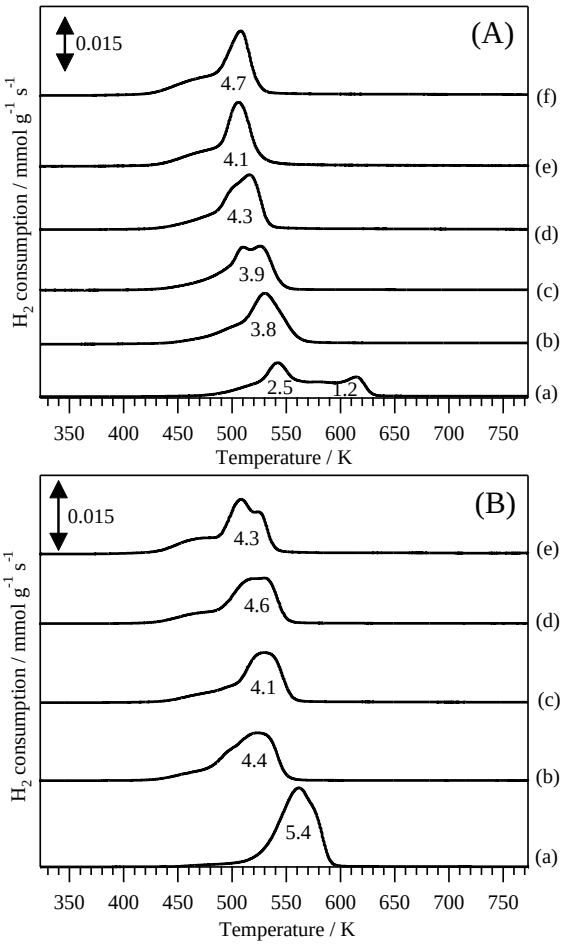

Fig. 8 H_2-TPR profiles of (A) CP-Cu-Al-O_x and (B) IMP-Cu-Al-O_x before and after DSS-like operations. After (a) calcination, (b) reduction, (c) 1st, (d) 10th (e) 20th, (f) 50th cycles of DSS-like operations. Each number indicates the amount of H_2 consumption (mmol g^{-1}) at the peak. Oxidation at 573 K under O_2 flow was held as a pretreatment in all samples.

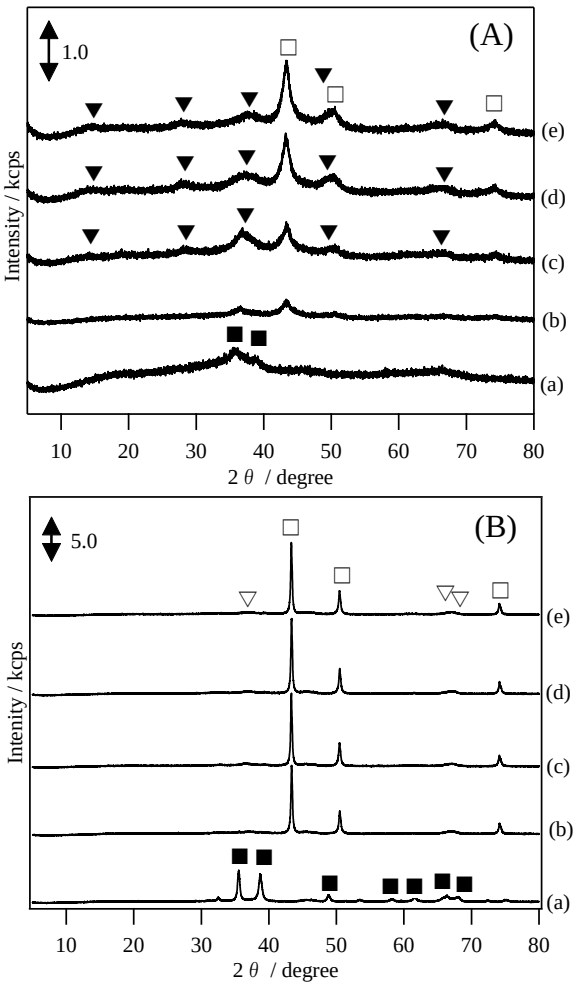

Fig. 9 XRD patterns of (A) CP-Cu-Al-O_x and (B) IMP-Cu-Al-O_x during 1 cycle of DSS-like operation. The dialog and sampling points (a)-(e) are described in Figure 1. (Close square) CuO, (open square) Cu, (close triangle) AlOOH (boehmite), and (open triangle) γ-Al_2O_3.

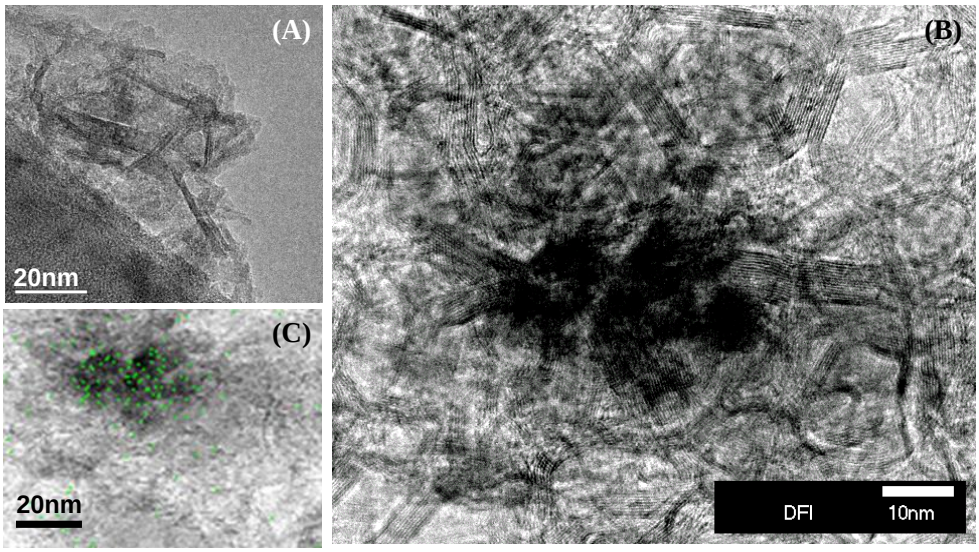

Fig. 10 Morphology of CP-catalyst after DSS-like operations analyzed by (A) HR-TEM, (B) STEM and (C) STEM-EDS. The green spots in (C) correspond to the presence of Cu.

8A(c) to (f)). These results suggested that the CuOs in the CP-catalyst were gradually dispersed on the catalyst by repeating DSS-like operations.[42,43] On the other hand, calcined IMP-catalyst had a single peak around 560 K (Figure 8B(a)). After reduction and DSS-like operations, the reduction peak was placed around 520 K with a small shift to higher temperature indicating the slight increase of the crystallinity of CuO.[44,45] According to these results, the easily reducible Cu species are related to the superior activity for the WGS reaction, and the superior nature of the CP-catalyst against DSS-like operations is not only related to the easy oxidation (supported by XAFS studies) but also easy reduction (indicated with H_2-TPR profiles) of Cu species. The importance of the redox behavior of Cu active species has also investigated in various reactions.[42,46,47] As the previous reports in WGS reaction, two plausible mechanisms over the Cu-based catalyst have been proposed. The redox mechanism via Cu^0 and Cu^+ changing on the surface of $Cu/ZnO/Al_2O_3$ catalyst have been reported.[9,11,15,36,48] On the other hand, the associative mechanism (intermediate formation such as formate, carbonate or carboxyl) was also discussed.[49,50] A more understanding of the correlation between the redox properties of Cu particles and the catalysis for WGS reaction over Cu-Al-O_x catalyst is the subject of a future investigation.

According to the previous reports, the *in-situ* formation of AlOOH during DSS-like operations is strongly associated with the high durability of the CP-catalyst.[24,25] However, the formation mechanism of the boehmite and the morphology between formed boehmite and Cu species still remain open questions. To study the boehmite formation process, the structure changes during 1 cycle of DSS-like operation investigated by XRD analysis is shown in Figure 9. The dialog and sampling points for this experiment are described in Figure 1 denoted as (a)-(e). In the case of CP-catalyst, small and broad peaks corresponding to CuO crystalline in the calcined catalyst (Figure 9A(a)) and Cu metal after reduction (Figure 9A(b)) were obtained. Thereafter, the diffractions resulting from formation of boehmite appeared during and after DSS-like operations (Figure 9A(c)-(e)). These results suggested that the boehmite was formed by exposure of amorphous alumina in steam. Some studies reported the preparation method of boehmite under steam rich conditions.[51-54] Intensity of the XRD patterns of boehmite at (130) peak at $2\theta = 38.5^o$ and BET surface area were gradually increased by repeating DSS-like operations, and their tendencies were well fitted with that of CO conversion (Figures S6(A) and (B)) suggesting the formation of boehmite strongly affected the increases in the catalytic activity. On the other hand, in the case of IMP-catalyst, sharp and strong peaks corresponding to large crystalline domains of CuO and Cu metal were observed after calcination and reduction, respectively (Figure 9B(a), (b)). Comparing the peaks after DSS-like operations, few changes on the large Cu metal and Al_2O_3 were observed (further details are shown in Figure S5(B)). It was found from XRD data that the CP-catalyst had smaller Cu metal particles than the IMP-catalyst, and the progressive changes of catalytic structure occurred only in the CP-catalyst accompanied with *in-situ* boehmite formation by repeating DSS-like operations.

HRTEM and STEM-EDX analyses were carried out for the CP-catalyst after DSS-like operations to study the morphology between boehmite and Cu particles. Figure 10 shows the HRTEM and STEM images of CP-catalyst after DSS-like operations with element analysis by EDS measurement. The presence of a needle-like structure owing to boehmite formation[52,54,55] was supported by the HRTEM image after DSS-like operations (Figure 10A). Using the STEM-EDS analysis of the catalyst, small Cu particles were surrounded by the needle-like structure in the CP-catalyst after DSS-like operations (Figures 10B and 10C). The needle-like boehmite structures and small Cu particles were observed in many places (*ex.* see Figure S7). According to these results, the needle-like boehmite was formed by repeating steam treatments under the DSS-like operations, and they stabilized the small redoxable Cu particles.

Conclusions

We investigated the dynamic behavior of Cu-Al-O_x catalyst during DSS-like operations using *in-situ* XAFS method in combination with other analytical techniques in order to reveal the novel properties of the durable Cu-Al-Ox catalyst and deactivation mechanism under DSS operations. The CP-catalyst showed a high activity and durability over the WGS reaction with DSS-like operations. We concluded that the superior catalytic performance of CP-catalyst was attributed to the formation of a card-house structure of the boehmite, which surrounded and kept the small Cu particles stable against DSS operations. The *in-situ* XAFS studies under the DSS-like operations clearly indicated that the Cu-catalyst is exposed to the frequent oxidation/reduction atmosphere, and which caused the growth and/or aggregation of active Cu particles. Based on the dynamic behavior of Cu-Al-O_x catalysts during DSS-like operation, it is concluded that the inhibition of excess oxidation of Cu metal to Cu_2O and/or successive reduction of Cu_2O to Cu metal is a key factor for maintaining the activity of Cu-catalyst for WGS reaction. In addition, the amount of redoxable Cu species seemed to be strongly contributed to the high activity of Cu-catalyst. From these results (summarized in Table S2), we ascertained that one of the key points for creating a highly active and stable Cu-catalyst for WGS reaction against DSS operations is to coordinate the small-redoxable Cu particles with stable substrates such as boehmite in order to inhibit Cu aggregations.

Acknowledgements

TS acknowledges the Grant-in-Aid for Scientific Research for Young Researchers (B) (No. 19760545) under the Ministry of Education, Culture, Sports Science and Technology (MEXT) of Japan. A part of this work is supported by the New Energy and Industrial Technology Development Organization (NEDO) in Japan. XAFS measurements were performed at the BL01B1 of SPring-8 with the approval of the Japan Synchrotron Radiation Research Institute (JASRI) (Proposal No. 2008A1170, 2009A1662 and 2009B1690).

Notes and references

[1] *School of Materials Science, Japan Advanced Institute of Science and Technology (JAIST), 1-1 Asahidai, Nomi, Ishikawa 923-1292, Japan.*
[2] *Department of Molecular Engineering, Graduate School of Engineering, Kyoto University, Katsura, Nishikyo-ku, Kyoto 615-8510, Japan. Fax: +81-75-383-2561; Tel: +81-75-383-2559; E-mail: shishido@moleng.kyoto-u.ac.jp*
[3] *Precursory Research for Embryonic Science and Technology (PRESTO), Japan Science and Technology Agency (JST),4-1-8 Honcho, Kawaguchi, Saitama 332-0012, Japan.*
[4] *Department of Chemical System Engineering, School of Engineering, The University of Tokyo, 7-3-1 Hongo, Bunkyo-ku, Tokyo 113-7656, Japan.*

† Electronic Supplementary Information (ESI) available: [Changes of EXAFS spectra, CN numbers, Cu(111) crystalline sizes, BET surface areas, and STEM-EDS mappings.]. See DOI: 10.1039/b000000x/

1 D. L. Trimm, *Appl. Catal. A: Gen.*, 2005, **296**, 1.
2 C. H. Kim, L. T. Thompson, *J. Catal.*, 2005, **230**, 66.
3 X. Liu, W. Ruettinger, X. Xu, R. Farrauto, *Appl. Catal. B: Env.*, 2005, **56**, 69.
4 Q. Fu, W. Deng, H. Saltsburg, M. Flytzani-Stephanopoulos, *Appl. Catal. B: Env.*, 2005, **56**, 57.
5 J. M. Zalc, V. Sokolovskii, D. G. Loffler, *J. Catal.*, 2002, **206**, 169.
6 W. Deng, M. Flytzani-Stephanopoulos, *Angew. Chem. Int. Ed.*, 2006, **45**, 2285.
7 X. Zhu, T. Hoang, L. Lobban, R. G. Mallinson, *Catal. Lett.*, 2009, **129**, 135.
8 R. Kam, J. Scott, R. Amal, C. Selomulya, *Chem. Eng. Sci.*, 2010, **65**, 6461.
9 M. J. L. Gines, N. Amadeo, M. Laborde, C. R. Apesteguia, *Appl. Catal. A: Gen.*, 1995, **131**, 283.
10 C. -S. Chen, W. -H. Cheng, S. -S. Lin, *Appl. Catal. A: Gen.*, 2003, **238**, 55.
11 T. Shishodo, M. Yamamoto, I. Atake, D. Li, Y. Tian, H. Morioka, M. Honda, T. Sano, K. Takehira, *J. Mol. Catal. A: Chem.*, 2006, **253**, 270.
12 J. Wu, M. Saito, *J. Catal.*, 2000, **195**, 420.
13 H. Yahiro, K. Murawaki, K. Saiki, T. Yamamoto, H. Yamaura, *Catal. Today*, 2007, **126**, 436.
14 T. Shishido, Y. Yamamoto, H. Morioka, K. Takai, K. Takehira, *Appl. Catal. A: Gen.*, 2004, **263**, 249.
15 Y. Tanaka, T. Utaka, R. Kikuchi, K. Sasaki, K. Eguchi, *Appl. Catal. A: Gen.*, 2003, **238**, 11.
16 H. Yahiro, K. Nakaya, T. Yamamoto, K. Saiki, H. Yamamura, *Catal. Commun.*, 2006, **7**, 228.
17 Y. Tanaka, T. Utaka, R. Kikuchi, K. Sasaki, K. Eguchi, *Appl. Catal. A: Gen.*, 2003, **242**, 287.
18 Y. Tanaka, T. Utaka, R. Kikuchi, T. Takeguchi, K. Sasaki, K. Eguchi, *J. Catal.*, 2003, **215**, 271.
19 Y. Tanaka, T. Takegucho, T. Kikuchi, K. Eguchi, *Appl. Catal. A: Gen.*, 2005, **279**, 59.
20 P. -J. Guo, L. -F. Chen, G. -B. Yu, Y. Zhu, M. -H. Qiao, H. -L. Xu, K. -N. Fan, *Catal. Commun.*, 2009, **10**, 1252.
21 P. Guo, L. Chen, Q. Yang, M. Qiao, H. Li, H. Li, H. Xu, K. Fan, *Int. J. Hydrogen Energy*, 2009, **34**, 2361.
22 O. Ilinich, W. Ruettinger, X. Liu, R. Farrauto, *J. Catal.*, 2007, **247**, 112.
23 W. Ruettinger, O. Ilinich, R. J. Farrauto, *J. Power Sour.*, 2003, **118**, 61.
24 S. Nishimura, T. Shishido, K. Ebitani, K. Teramura, T. Tanaka, *Appl. Catal. A: Gen.*, 2010, **387**, 185.
25 T. Shishido, S. Nishimura, Y. Yoshinaga, K. Ebitani, K. Teramura, T. Tanaka, *Catal. Commun.*, 2009, **10**, 1057.
26 D. mendes, H. Garcia, V. B. Silva, A. Mendes, L. M. Madeira, *Ind. Eng. Chem. Res.*, 2009, **48**, 430.
27 I. Kasatkin, P. Kurr, B. Kniep, A. Trunschke, R. Schlogl, *Angew. Chem. Int. Ed.*, 2007, **46**, 7324.
28 S. Patel, K. K. Pant, *J. Power Sources*, 2006, **159**, 139.
29 J. W. Evans, M. S. Wainwright, A. J. Bridgewater, D. J. Young, *Appl. Catal.*, 1983, **7**, 75.
30 J. R. Jensen, T. Johannessen, H. Livbjerg, *Appl. Catal. A: Gen.*, 2004, **266**, 117.
31 A. Suzuki, M. Nomura, *Proceedings of 9th Jpn. XAFS Soc. Annu. Meeting*, 7O08.
32 T. Shido, A. Yamaguchi, Y. Inada, K. Asakura, M. Nomura, Y. Iwasawa, *Top. Catal.*, 2002, **18**, 53.
33 M. M. Gunter, T. Ressler, R. E. Jentoft, B. Bems, *J. Catal.*, 2001, **203**, 133.
34 J. Stotzel, D. Lutzenkirchen-Hecht, R. Frahm, B. Kimmerle, A. Baiker, M. J. Beier Nachtegaal, J. -D. Grunwaldt, *J. Phys.: Conf. Ser.*, 2009, **190**, 012153.
35 S. Nishimura, A. Takagaki, S. Maenosono, K. Ebitani, *Langmuir*, 2010, **26**, 4473.
36 T. Shishido, M. Yamamoto, D. Li, Y. Tian, H. Morioka, M. Honda, T. Sano, K. Takehira, *Appl. Catal. A: Gen.*, 2006, **303**, 62.
37 K. Sekizawa, S. -I. Yano, K. Eguchi, H. Arai, *Appl. Acatal. A: Gen.*, 1998, **169**, 291.
38 C. S. Chen, C. C. Chen, T. W. Lai, J. H. Wu, C. H. Chen, J. F. Lee, *J. Phys. Chem. C*, 2011, **115**, 12891.

39 G. -C. Wang, S. -X. Tao, X. -H. Bu, *J. Catal.*, 2006, **244**, 10.

40 The easily-oxidized Cu concentration (Cu^{+}/Cu^{0}_{total}) during 1 cycle of DSS-like operation in the fresh CP-catalyst was estimated to be 3.76×10^{-1} in the Figure 5(A) under the condition with 323 K of the steam cycle, whereas that was 3.56×10^{-1} in the Figure S4 using 353 K of the steam cycle. Furthermore, the oxidation feature during DSS-like operation looks similar; *i.e.* no changes were caused by the differennces between 323 and 353K.

41 D. F. Shriver, P. W. Atkins, "Inorganic Chemistry 3e", Oxford Univ. Press, 1999.

42 J. Agrell, H. Birgersson, M. Boutonnet, I. Melian-Cabrera, R. M. Navarro, J. L. G. Fierro, *J. Catal.*, 2003, **219**, 389.

43 M. -F. Luo, P. Fang, M. He, Y. -L. Xie, *J. Mol. Catal. A: Chem.*, 2005, **239**, 243.

44 S. -K. Kim, K. -H. Kim, S. -K. Ihm, *Chemosphere*, 2007, **68**, 287.

45 K. V. R. Chary, K. K. Seela, D. Naresh, P. Ramakanth, *Catal. Commun.*, 2008, **9**, 75.

46 M. Vijayaraj, C. S. Gopinath, *J. Catal.*, 2006, **241**, 83.

47 S. Velu, K. Suzuki, C. S. Gopinath, H. Yoshida, T. Hattori, *Phys. Chem. Chem. Phys.*, 2002, **4**, 1990.

48 C. -S. Chen, T. -W. Lai, C. -C. Chen, *J. Catal.*, 2010, **273**, 18.

49 A. A. Golhale, J. A. Dumesic, M. Mavrikakis, *J. Am. Chem. Soc.*, 2008, **130**, 1402.

50 J. L. C. Fajin, M. Natalia, D. S. Cordeiro, F. Illas, J. R. B. Gomes, *J. Catal.*, 2009, **268**. 131.

51 R. S. Gates, S. M. Hus, E. E. Klaus, *Tribology Trans.*, 1989, **32**, 357.

52 X. Y. Chen, S. W. Lee, *Chem. Phys. Lett.*, 2007, **438**, 279.

53 Y. Hakuta, H. Ura, H. Hayashi, K. Arai, *Mater. Chem. Phys.*, 2005, **93**, 466.

54 W. H. Kim, I. S. Park, J. Park, *Organic. Lett.*, 2006, **8**, 2543.

55 Y. Zhao, R. L. Frost, *J. Coll. Int. Sci.*, 2008, **326**, 289.